Acta Cryst. (1975). B31, 1879

Structure Block Stacking in Intermetallic Compounds. I. The Rhombohedral-Hexagonal $M_{n+1}X_{5n-1}$ and the Monoclinic-Hexagonal-Trigonal-Orthorhombic $M_{n+1}X_{5n+2}$ Structure Series*

BY E. PARTHÉ AND R. LEMAIRE

Laboratoire de Cristallographie aux Rayons X, Université de Genève, 32 Bd. d'Yvoy, CH-1211 Geneva 4, Switzerland and Laboratoire de Magnétisme, CNRS, B.P. 166, F-38042 Grenoble, France

(*Received* 18 *February* 1975; *accepted* 21 *February* 1975)

In binary systems containing rare-earth elements (M) and transition elements (X) several intermetallic compounds with composition between MX_2 and MX_5 are formed which, according to their mechanical properties, fall into two groups. The brittle alloys are hexagonal or rhombohedral and belong to the $M_{n+1}X_{5n-1}$ structure series. This series may be considered to be formed by stacking M_2X_4 blocks (characteristic of Laves phases) with a varying number of MX_5 blocks (characteristic of the Haucke phase $CaCu_5$). The soft alloys with pronounced cleavage have monoclinic symmetry. They belong to a new $M_{n+1}X_{5n+2}$ structure series which contains a new structure block, M_2X_7, found in the Zr_2Ni_7 structure. A consideration of the intraplanar translation vectors and of the possible rotations of the M_2X_7 blocks shows that this structure series has three other subseries apart from the monoclinic Zr_2Ni_7 subseries, these being hexagonal, trigonal and orthorhombic. Point positions for these hypothetical structures are given together with a ready method of recognizing their presence from precession photographs.

Introduction

We consider binary intermetallic systems M–X for which M is Mg, Ca, group 3 or 4 elements, rare-earth elements or actinides and X is Fe, Co, Ni, Cu or Zn. Compounds with compositions between MX_2 and MX_5 are often found in these systems and have structures related to the Laves MX_2 and Haucke MX_5 phases. Data for these structure types have been compiled in Table 1. Among the ten hexagonal, rhombohedral and monoclinic known structure types only the hexagonal and rhombohedral structures are fairly well understood and have been grouped into a structure series. This paper is an attempt to classify all these structure types and to propose new structures for related structure series. The results presented will be useful for the quick solution of unknown crystal structures of other compounds within this composition range.

Previous results

The relationship between the hexagonal and rhombohedral structure types has been discussed by Cromer & Larson (1959), Lemaire (1966) and Khan (1974*a*,*b*).

Cromer & Larson have reported that the $CeNi_3$, $PuNi_3$ and Ce_2Ni_7 types can be obtained by alternate stacking of MX_2 and MX_5 layers. They also elaborated a different description in which these structure types are based only on the hexagonal $CaCu_5$ structure type. By introducing ordered substitutions of M atoms in the twofold X position of the MX_5 structure, followed by appropriate shifts of layers and small displacements of adjacent M atoms along **c**, they could derive all the hexagonal and rhombohedral structure types.

Lemaire has also proposed this substitution scheme and has formulated equations expressing the substitution mechanism for the different structure types.

Khan has noted that the substitution scheme for the

Table 1. *Structure types for compounds with compositions between* MX_2 *and* MX_5

Hexagonal-rhombohedral series		
66·7 % X	$MgZn_2$:	$P6_3/mmc$, $c/a \simeq 2\sqrt{2/3}$, $Z=4$ *Strukturbericht*, **1**, 180, 228
	$MgCu_2$:	$(Fd3m) \rightarrow R\bar{3}m$, $c/a = 3\sqrt{2/3}$, $Z=6$ (triple hex. cell) *Strukturbericht*, **1**, 490, 531
75·0 %X	$CeNi_3$:	$P6_3/mmc$, $c/a \simeq 4\sqrt{2/3}$, $Z=6$ Cromer & Olson (1959)
	$PuNi_3$ or $NbBe_3$:	$R\bar{3}m$, $c/a \simeq 6\sqrt{2/3}$, $Z=9$ (triple hex. cell) Cromer & Olsen (1959) Sands, Zalkin & Krikorian (1959)
77·8 % X	Ce_2Ni_7:	$P6_3/mmc$, $c/a \simeq 6\sqrt{2/3}$, $Z=4$ Cromer & Larson (1959)
	Gd_2Co_7 or Er_2Co_7:	$R\bar{3}m$, $c/a \simeq 9\sqrt{2/3}$, $Z=6$ (triple hex. cell) Bertaut, Lemaire & Schweizer (1965) Ostertag (1967)
79·0 % X	Sm_5Co_{19}:	$P6_3/mmc$, $c/a \simeq 8\sqrt{2/3}$, $Z=2$ Khan (1974*b*)
	Ce_5Co_{19}:	$R\bar{3}m$, $c/a \simeq 12\sqrt{2/3}$, $Z=3$ (triple hex. cell) Khan (1974*a*)
Monoclinic structure types		
77·8 % X	Zr_2Ni_7:	$C2/m$ Eshelman & Smith (1972)
80·0 % X	$PuNi_4$:	$C2/m$ Cromer & Larson (1960)

* Part II will deal with experimental structure determinations in rare-earth–nickel systems and will be submitted to *Acta Crystallographica* for publication.

derivation of these structure types appears very simple but that the determination of the atomic positions for a particular structure type is quite laborious. He then described a procedure by which the lattice parameters and atomic positions for any of the hexagonal and rhombohedral structure types could be easily calculated. Khan's scheme reverts to the earlier notion of Cromer & Larson of MX_2 and MX_5 layers. The structures are considered to be divided into blocks of MX_2 as in the Laves phases and blocks of MX_5 as in $CaCu_5$. The various structure types differ in the ratio of the number of blocks MX_2 to the number of blocks MX_5.

No such construction scheme has been found for the two monoclinic structure types. These are layered along a pseudo hexagonal axis somewhat inclined towards the monoclinic c_M axis. A rather complicated mechanism has been proposed by Eshelman & Smith (1972) to show that the Zr_2Ni_7 structure may be derived from the $CaCu_5$ structure by removal of a layer of X atoms, collapse of the remaining structure and shifts of atoms. No clear relationship between the Zr_2Ni_7 and the $PuNi_4$ type has been formulated.

The three structure blocks

The idea of structure blocks as used by Khan for the hexagonal-rhombohedral structure series may be generalized. The principal structure blocks which form the hexagonal-rhombohedral series will be redefined and a new block will be proposed which allows the Zr_2Ni_7 and $PuNi_4$ structure types to be grouped into a new monoclinic-hexagonal-trigonal-orthorhombic structure series.

Three structure blocks form the building elements in the two series: an M_2X_4, an M_2X_7, and an MX_5 block. A stacking of M_2X_4 blocks with increasing number of MX_5 blocks allows the construction of the crystal structure types of the rhombohedral-hexagonal $M_{n+1}X_{5n-1}$ series, n being any positive integer [$M_2X_4+(n-1)MX_5$: $MX_2, MX_3, M_2X_7, M_5X_{19}, MX_4, \ldots, MX_5$]. Alternation of M_2X_7 blocks with increasing number of MX_5 blocks permits the construction of the crystal structure types of the monoclinic-hexagonal-trigonal-orthorhombic $M_{n+1}X_{5n+2}$ series [$M_2X_7+(n-1)MX_5$: $M_2X_7, MX_4, M_4X_{17}, \ldots, MX_5$]. Each structure series has subseries which differ only in the relative orientation of the structure blocks and in the symmetry of the types. The $M_{n+1}X_{5n-1}$ series presents a hexagonal and a rhombohedral subseries, and the $M_{n+1}X_{5n+2}$ series monoclinic, hexagonal, trigonal and orthorhombic subseries.

The three structure blocks are shown in Fig. 1. They can be described in a hexagonal unit cell (a_{BL}, c_{BL}) or in the corresponding orthohexagonal cell (a_{OH}, b_{OH}, c_{OH}). The idealized point positions and projections of the blocks along $\mathbf{c}_{BL}$ and $\mathbf{a}_{OH}$ or $\mathbf{b}_{OH}$ are given in Figs. 2(*a*), 2(*b*) and 2(*c*). The bottom and top X layers of all blocks are identical, except for a possible intraplanar translation. If two blocks are stacked one on top of the other, such an X layer will be common to both structure blocks; it may be regarded as a welding layer and will be denoted by *W*. In the different blocks there are three kinds of intermediate layers: *I*, *I'* and *I''*.

The MX_5 block corresponds to the $CaCu_5$ structure type. Such a block can be considered as an alternate succession of two different layers, a *W* and an *I* layer

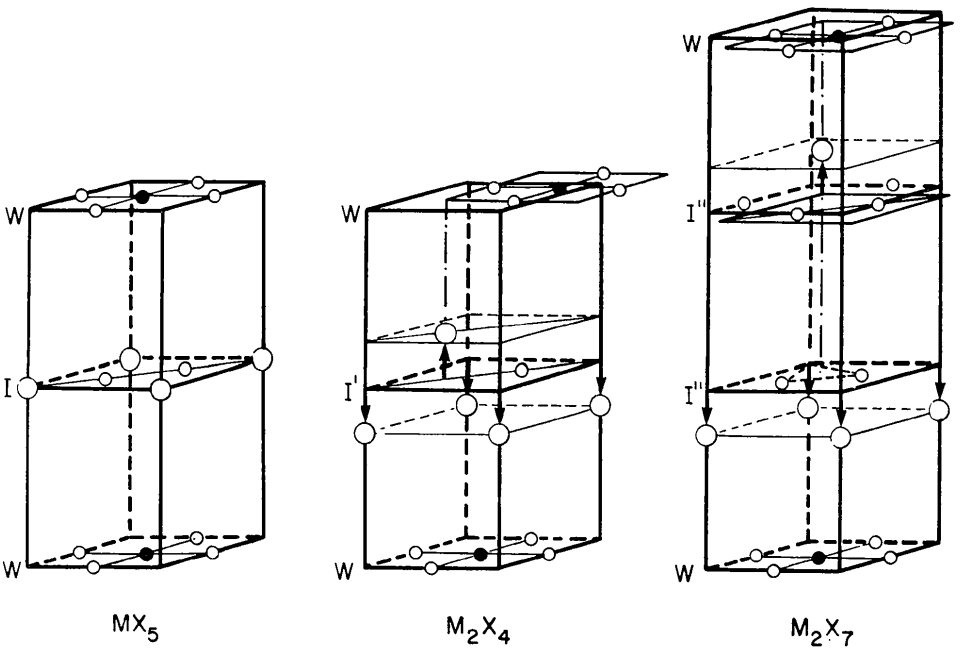

Fig. 1. Schematic drawing of the three structure blocks where for reasons of clear presentation the *c*/*a* ratio is three times larger than the real one. X atoms are shown as small circles, M atoms as large circles.

Table 2. *The relative unit-cell dimensions for both structures series referred to* $\mathbf{a}_{BL}$, *the hexagonal basis vector of the structure blocks*

$M_{n+1}X_{5n-1}$ series	Relative height of minimum block sequence	$M_{n+1}X_{5n+2}$ series
$h=n\dfrac{\sqrt{2}}{\sqrt{3}}\cdot\lvert\mathbf{a}_{BL}\rvert$		$h=\dfrac{2n\sqrt{6}+\sqrt{5}}{6}\cdot\lvert\mathbf{a}_{BL}\rvert$

Rhombohedral subseries $R\bar{3}m$ (No. 166)	Hexagonal subseries $P6_3/mmc$ (No. 194)	Monoclinic subseries $C2/m$ (No. 12)	Hexagonal subseries $P6_122$ (No. 178)	Trigonal subseries $P3_112$ (No. 151)	Orthorhombic subseries $Ccmm$ (No. 63)
$\mathbf{a}_{TH}=\mathbf{a}_{BL}$ $\mathbf{c}_{TH}=3h$	$\mathbf{a}_H=\mathbf{a}_{BL}$ $\lvert\mathbf{c}_H\rvert=2h$	$\mathbf{a}_M=-\mathbf{a}_{OH}$, $\lvert\mathbf{a}_M\rvert=\lvert\mathbf{a}_{BL}\rvert$ $\mathbf{b}_M=-\mathbf{b}_{OH}$, $\lvert\mathbf{b}_M\rvert=\lvert\mathbf{a}_{BL}\rvert\cdot\sqrt{3}$	$\mathbf{a}_H=\mathbf{a}_{BL}$ $\lvert\mathbf{c}_H\rvert=6h$	$\mathbf{a}_{TR}=\mathbf{a}_{BL}$ $\lvert\mathbf{c}_{TR}\rvert=3h$	$\mathbf{a}_O=\mathbf{a}_{OH}$, $\lvert\mathbf{a}_O\rvert=\lvert\mathbf{a}_{BL}\rvert$ $\mathbf{b}_O=\mathbf{b}_{OH}$, $\lvert\mathbf{b}_O\rvert=\lvert\mathbf{a}_{BL}\rvert\cdot\sqrt{3}$
(referred to triple hexagonal unit-cell) $\dfrac{c_{TH}}{a_{TH}}=3n\dfrac{\sqrt{2}}{\sqrt{3}}$	$\dfrac{c_H}{a_H}=2n\dfrac{\sqrt{2}}{\sqrt{3}}$	$\lvert\mathbf{c}_M\rvert=\sqrt{\left[h^2+\left(\dfrac{a_{BL}}{3}\right)^2\right]}$ $\tan(\beta_M-90°)=\dfrac{\lvert\mathbf{a}_{BL}\rvert}{3h}$	$\dfrac{c_H}{a_H}=2n\sqrt{6}+\sqrt{5}$	$\dfrac{c_{TR}}{a_{TR}}=\dfrac{2n\sqrt{6}+\sqrt{5}}{2}$	$\dfrac{|c_O|}{a_O}=2h$ $\dfrac{c_O}{a_O}=\dfrac{2n\sqrt{6}+\sqrt{5}}{3}$

The latter is composed of the two kinds of atoms in the proportion of one M to two X. The M atoms are located at the centres of hexagons formed by the X atoms. The ideal axial ratio $c_{BL}/a_{BL}=\sqrt{2}/\sqrt{3}$ has been obtained by assuming equal X–X distances.

The M_2X_4 and M_2X_7 blocks, which are richer in M atoms than the MX_5, can also be constructed with *W* and *I* layers. The M_2X_4 block is the building element of the Laves phases. The succession of the layers is the same as in the MX_5 block, but one of the two X atoms in the intermediate layer is replaced by an M atom. Adjacent rare-earth atoms would then be too close to each other and are thus shifted by $\frac{1}{8}c$ parallel to **c** on opposite sides of their original layer, in which only the unsubstituted X atom remains. The top welding layer is translated by $\mathbf{T}_{M_2X_4}=\frac{1}{3}\mathbf{a}_{BL}-\frac{1}{3}\mathbf{b}_{BL}$ (referred to hexagonal axes) or $\mathbf{T}_{M_2X_4}=\frac{1}{3}\mathbf{b}_{OH}$ (referred to orthohexagonal axes) with respect to the bottom one in order to achieve close packing. The ideal c_{BL}/a_{BL} ratio of the block is

Fig. 2 (*a*). MX_5 block. (i) Projection along $\mathbf{c}_{OH}$ or $\mathbf{c}_{BL}$. (ii) Projection along $\mathbf{a}_{OH}$ (black circles with $x=0$). (iii) Projection along $\mathbf{b}_{OH}$ (black circles with $y=0$).

Point positions

(*a*) Referred to hexagonal axes (a_{BL}, c_{BL}, $c_{BL}/a_{BL}=\sqrt{2}/\sqrt{3}$)

$\frac{3}{2}$X: $\frac{1}{2}01$, $0\frac{1}{2}1$, $\frac{1}{2}\frac{1}{2}1$
1M: $00\frac{1}{2}$
2X: $\frac{2}{3}\frac{1}{3}\frac{1}{2}$, $\frac{1}{3}\frac{2}{3}\frac{1}{2}$
$\frac{3}{2}$X: $\frac{1}{2}00$, $0\frac{1}{2}0$, $\frac{1}{2}\frac{1}{2}0$

(*b*) Referred to orthohexagonal axes ($a_{OH}=a_{BL}$, $b_{OH}=a_{BL}\cdot\sqrt{3}$, $c_{OH}=c_{BL}$)

$\frac{6}{2}$X: $0\frac{1}{2}1$, $\frac{1}{4}\frac{1}{4}1$, $\frac{1}{4}\frac{3}{4}1$
2M: $00\frac{1}{2}$
4X: $0\frac{1}{3}\frac{1}{2}$, $0\frac{2}{3}\frac{1}{2}$
$\frac{6}{2}$X: $0\frac{1}{2}0$, $\frac{1}{4}\frac{1}{4}0$, $\frac{1}{4}\frac{3}{4}0$

$+[\frac{1}{2}\frac{1}{2}0]$

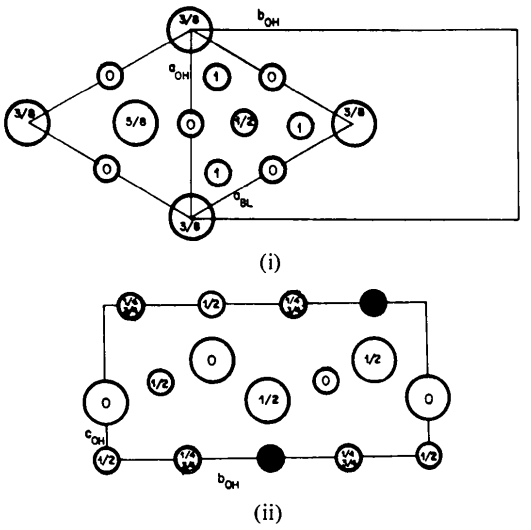

Fig. 2 (*b*). M_2X_4 block. (i) Projection along $\mathbf{c}_{OH}$ or $\mathbf{c}_{BL}$. (ii) Projection along $\mathbf{a}_{OH}$ (black circles with $x=0$).

Point positions

(*a*) Referred to hexagonal axes (a_{BL}, c_{BL}, $c_{BL}/a_{BL}=\sqrt{2}/\sqrt{3}$)

$\frac{3}{2}$X: $\frac{1}{3}\frac{1}{6}1$, $\frac{5}{6}\frac{1}{6}1$, $\frac{5}{6}\frac{2}{3}1$

1M: $\frac{1}{3}\frac{2}{3}\frac{5}{8}$

1X: $\frac{2}{3}\frac{1}{3}\frac{1}{2}$

1M: $00\frac{3}{8}$

$\frac{3}{2}$X: $\frac{1}{2}00$, $0\frac{1}{2}0$, $\frac{1}{2}\frac{1}{2}0$

(*b*) Referred to orthohexagonal axes ($a_{OH}=a_{BL}$, $b_{OH}=a_{BL}\cdot\sqrt{3}$, $c_{OH}=c_{BL}$)

$\frac{6}{2}$X: $0\frac{5}{6}1$, $\frac{1}{4}\frac{7}{12}1$, $\frac{1}{4}\frac{1}{12}1$

2M: $0\frac{1}{3}\frac{5}{8}$

2X: $0\frac{2}{3}\frac{1}{2}$

2M: $00\frac{3}{8}$

$\frac{6}{2}$X: $0\frac{1}{2}0$, $\frac{1}{4}\frac{1}{4}0$, $\frac{1}{4}\frac{3}{4}0$

$+[\frac{1}{2}\frac{1}{2}0]$

$\sqrt{2}/\sqrt{3}$ as for the MX_5 block. In the M_2X_7 block, two intermediate layers are stacked one above the other; atoms of one layer and interstices of the second layer are superposed. The upper and lower halves of the M_2X_7 block are similar to those of the MX_5 block but they are translated with respect to each other by $\mathbf{T}_{M_2X_7}=-\frac{1}{3}\mathbf{a}_{BL}-\frac{1}{3}\mathbf{b}_{BL}$ (referred to hexagonal axes) or $\mathbf{T}_{M_2X_7}=\frac{1}{3}\mathbf{a}_{OH}$ (referred to orthohexagonal axes). In the middle of the block, adjacent rare-earth atoms would be too close; they are thus shifted by $\pm 0{\cdot}108c_{MX_5}$ along **c**. The idealized point positions and the relative block dimensions have been obtained by assuming equal X–X distances. Referring to hexagonal axes the c_{BL}/a_{BL} ratio is then $(2\sqrt{6}+\sqrt{5})/6$ for the M_2X_7 block, which means that this block is 1·456 times higher than the other two blocks.

For a stacking together of these three types of blocks one has to consider

(*a*) a possible intraplanar translation of the top welding layer with respect to the bottom welding layer of a block;

(*b*) a possible relative rotation of adjacent blocks. Since the top welding layer in the MX_5 block is exactly above the bottom welding layer, MX_5 blocks can be stacked without intraplanar translation: $\mathbf{T}_{MX_5}=0$. However as shown above in the M_2X_4 block the top welding layer is displaced by $\mathbf{T}_{M_2X_4}=\frac{1}{3}\mathbf{a}_{BL}-\frac{1}{3}\mathbf{b}_{BL}$ and in the M_2X_7 block by $\mathbf{T}_{M_2X_7}=-\frac{1}{3}\mathbf{a}_{BL}-\frac{1}{3}\mathbf{b}_{BL}$. Thus it is necessary to give proper displacements to adjacent

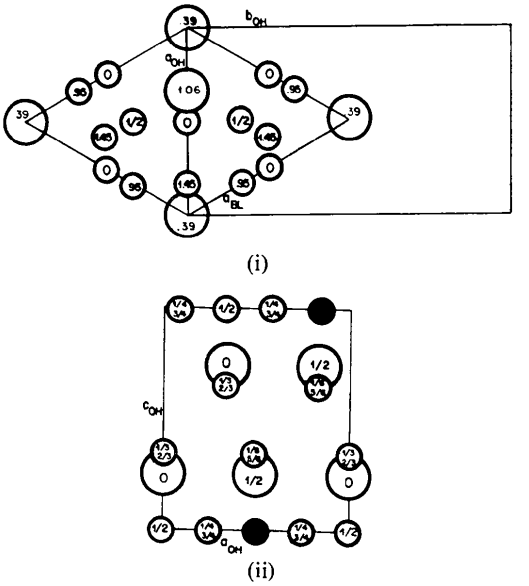

Fig. 2 (*c*). M_2X_7 block. (i) Projection along $\mathbf{c}_{OH}$ or $\mathbf{c}_{BL}$. (ii) Projection along $\mathbf{b}_{OH}$ (black circles with $y=0$).

Point positions (z value always being referred to MX_5 or M_2X_4 block height. For full height of block $z=1{\cdot}45_6$).

(*a*) Referred to hexagonal axes (a_{BL}, c_{BL}, $c_{BL}/a_{BL}=(2\sqrt{6}+\sqrt{5})/6$)

$c_{BL}/a_{BL}=1{\cdot}45_6\,.\,(c_{BL}/a_{BL})_{MX_5}$

$\frac{3}{2}$X: $\frac{1}{6}\frac{1}{6}1{\cdot}45_6$, $\frac{1}{6}\frac{2}{3}1{\cdot}45_6$, $\frac{2}{3}\frac{1}{6}1{\cdot}45_6$

1M: $\frac{2}{3}\frac{2}{3}1{\cdot}06_3$

2X: $\frac{1}{3}00{\cdot}95_5$, $0\frac{1}{3}0{\cdot}95_5$

2X: $\frac{1}{3}\frac{2}{3}\frac{1}{2}$, $\frac{2}{3}\frac{1}{3}\frac{1}{2}$

1M: $000{\cdot}39_3$

$\frac{3}{2}$X: $\frac{1}{2}00$, $0\frac{1}{2}0$, $\frac{1}{2}\frac{1}{2}0$

(*b*) Referred to orthohexagonal axes ($a_{OH}=a_{BL}$, $b_{OH}=a_{BL}\cdot\sqrt{3}$, $c_{OH}=c_{BL}$)

$\frac{6}{2}$X: $\frac{5}{6}01{\cdot}45_6$, $\frac{1}{12}\frac{1}{4}1{\cdot}45_6$, $\frac{1}{12}\frac{3}{4}1{\cdot}45_6$

2M: $\frac{1}{3}0\ 1{\cdot}06_3$

4X: $\frac{1}{3}\frac{2}{3}0{\cdot}95_5$, $\frac{1}{3}\frac{1}{3}0{\cdot}95_5$

4X: $0\frac{1}{3}\frac{1}{2}$, $0\frac{2}{3}\frac{1}{2}$

2M: $000{\cdot}39_3$

$\frac{6}{2}$X: $\frac{1}{2}00$, $\frac{1}{4}\frac{1}{4}0$, $\frac{1}{4}\frac{3}{4}0$

$+[\frac{1}{2}\frac{1}{2}0]$

blocks. To facilitate the correct description of the stacking of the structure blocks, reference atoms can be taken in the bottom and top X layers, the welding planes of the blocks. In the projections along a_{OH} or b_{OH} shown in Fig. 2(*a*), (*b*) and (*c*) these reference atoms are in the projection plane, *i.e.* at $x=0$ or $y=0$ respectively and are represented by black circles. The blocks always stack in such a way that the reference atoms lie in the middle of the projection of the bottom welding layer.

Since the welding layer has sixfold symmetry, rotation of any block by 0°, ±60°, ±120° and 180° brings its bottom welding layer into coincidence with the top welding layer of an underlying block. The MX_5 block has itself hexagonal symmetry, thus a rotation by ±60°, ±120° or 180° gives the same result as no rotation at all. If we consider two M_2X_4 blocks, a rotation of the top one by ±60° is the same as a rotation of 180°. Further, rotation by ±120° gives the same result as no rotation. Thus for the stacking of M_2X_4 blocks only two possibilities need to be considered, that is no

rotation or a rotation by 180° around c_{BL}. With the M_2X_7 blocks there are, however, four different possibilities corresponding to a rotation of the top block by 0°, ±60°, ±120° and 180°. The stacking of M_2X_4 and M_2X_7 blocks is schematically presented in Fig. 3.

The hexagonal-rhombohedral $M_{n+1}X_{5n-1}$ series

This structure series has already been discussed by Khan (1974*a*) assuming a stacking of blocks of different sizes.* In the rhombohedral subseries, the stacking of M_2X_4 blocks is described only by the intraplanar translation $\mathbf{T}_{M_2X_4}$ while in the hexagonal subseries successive M_2X_4 blocks are derived from one another by translation followed by a rotation of 180°. One example of this series, the structure of $PuNi_3$, will now be demonstrated in order to familiarize the reader with the various structure blocks defined in this paper. The block stacking for the rhombohedral $PuNi_3$ structure type is shown in Fig. 4. Since there is an alternation of MX_4 blocks with M_2X_5 blocks a projection along $\mathbf{a}_{OH}$ was chosen for the graphical representation. In this case the reference atoms of all the displaced structure blocks remain in the plane of projection. The individual atom parameters can be obtained easily with the help of Figs. 2(*a*) and 2(*b*).

For each structure type it is possible to formulate a minimum block sequence which leads to the complete structure after repeated stacking with the same orientation for the rhombohedral series, or alternate rotation of M_2X_4 block for the hexagonal subseries. For example, in the case of $PuNi_3$, the minimum block sequence consists of one M_2X_4 and one MX_5 block. The height h of this minimum block sequence is related to the composition of the $M_{n+1}X_{5n-1}$ compounds. The hexagonal or triple hexagonal cell dimensions are given in the left hand part of Table 2.

A graphical survey of structure types of the $M_{n+1}X_{5n-1}$ structure series is presented in Fig. 5. Here only contour lines of the structure blocks are shown. Referring to the projections along a_{OH} shown in Figs. 2(*a*) and 2(*b*), an MX_5 block may be represented by a rectangle and an M_2X_4 block by a parallelogram after joining the black reference atoms. To clarify the figure, 15 has been printed inside the MX_5 blocks and 24 inside the M_2X_4 blocks. If the sums of the printed numbers in the minimum block sequence are formed, first ciphers separately from the second ciphers, the two totals correspond to the overall composition formula for the particular structure type.

Other subseries can be constructed by assuming more complex stacking sequences of the M_2X_4 blocks. For example in the Laves phases other than $MgZn_2$ and $MgCu_2$, at least five other stackings are known. In the case of $MgNi_2$, the M_2X_4 blocks are alternately rotated by 0° and 180°.

The monoclinic subseries of the $M_{n+1}X_{5n+2}$ structure series

A study of the Zr_2Ni_7 and $PuNi_4$ structure types reveals that these two types belong to the monoclinic subseries of a new series involving M_2X_7 blocks and MX_5 blocks.

* Khan has given for this structure series the different general formula $RT_{(5n+4)/(n+2)}$, n being zero or any positive integer.

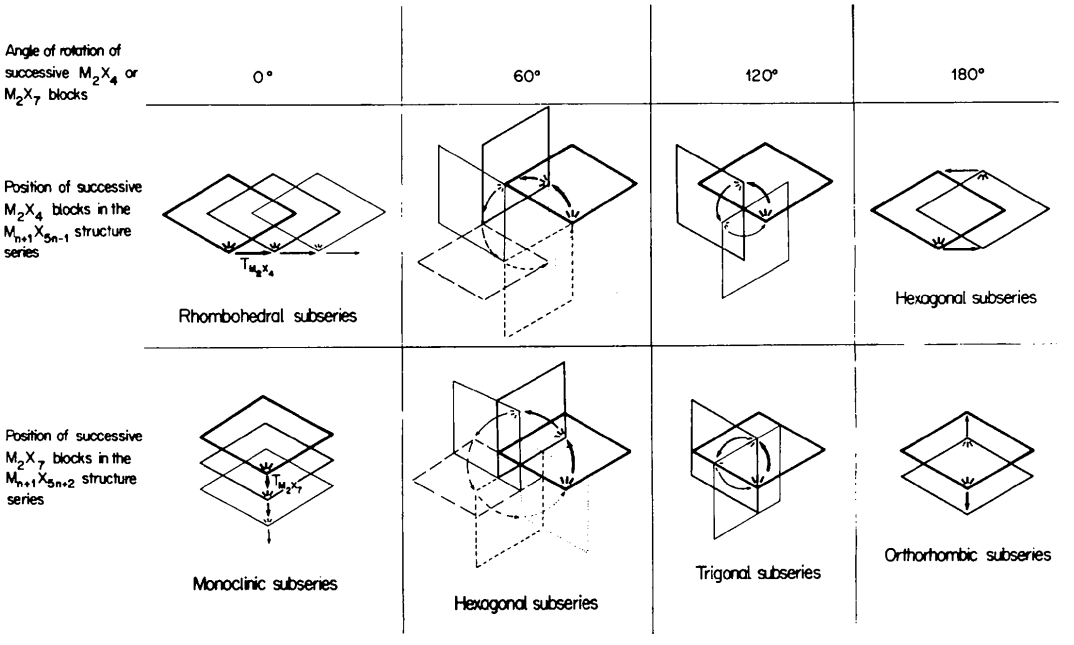

Fig. 3. The different possibilities of stacking of M_2X_4 and M_2X_7 blocks.

Table 3. *Structure data for* Zr_2Ni_7 *after Eshelman & Smith* (1972) *together with modified data which permit a transformation to a smaller unit cell*

$C2/m$ (No. 12), $Z=4$
$a_{ES}=4{\cdot}698$, $b_{ES}=8{\cdot}235$, $c_{ES}=12{\cdot}193$ Å, $\beta_{ES}=95{\cdot}83°$

	x	y	z
Zr in 4(*i*)	0·2115 → 0·221	0	0·6133 → 0·615
4(*i*)	0·2695 → 0·279	0	0·8840 → 0·885
Ni in 4(*i*)	0·2561 → ¼	0	0·2460 → ¼
8(*j*)	0·2075 → 0·205	0·1625 → 0·165	0·0762 → 0·078
8(*j*)	0·2974 → 0·295	0·1679 → 0·165	0·4208 → 0·422
8(*j*)	0·5033 → ½	0·2464 → ¼	0·2507 → ¼

The Zr_2Ni_7 type is the first member of this series and may be constructed by stacking M_2X_7 blocks alone. The block-stacking model for this structure type shows that it should be possible to describe this structure type with a unit cell of half the volume of the one given by Eshelman & Smith (1972). The structure data for Zr_2Ni_7 as published by Eshelman & Smith are summarized in Table 3. Allowing for small changes in the point positions of less than 0·05 Å a unit-cell transformation can be made which leads to a smaller monoclinic unit cell (a_M, b_M, c_M, β_M). The following vector relations may be written:

$$\mathbf{a}_M = -\mathbf{a}_{ES},\ \mathbf{b}_M = -\mathbf{b}_{ES},\ \mathbf{c}_M = \tfrac{1}{2}\mathbf{a}_{ES} + \tfrac{1}{2}\mathbf{c}_{ES}$$

from which follows:

$$|\mathbf{c}_M| = \tfrac{1}{2}\sqrt{(a_{ES}^2 + c_{ES}^2 + 2a_{ES}c_{ES}\cos\beta_{ES})}$$

and

$$\sin\beta_M = \tfrac{1}{2}\frac{c_{ES}}{c_M}\,.\,\sin\beta_{ES}\,.$$

The new structure data for the Zr_2Ni_7 type are summarized in Table 4. The origin of the new small unit cell has been shifted by $00\frac{1}{2}$ so that the (001) plane is a welding plane for the structure blocks and a block

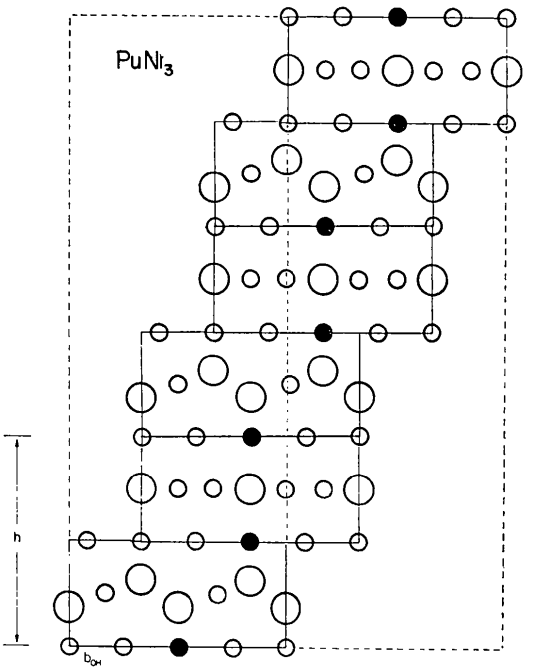

Fig. 4. Block stacking for the rhombohedral $PuNi_3$ structure type.

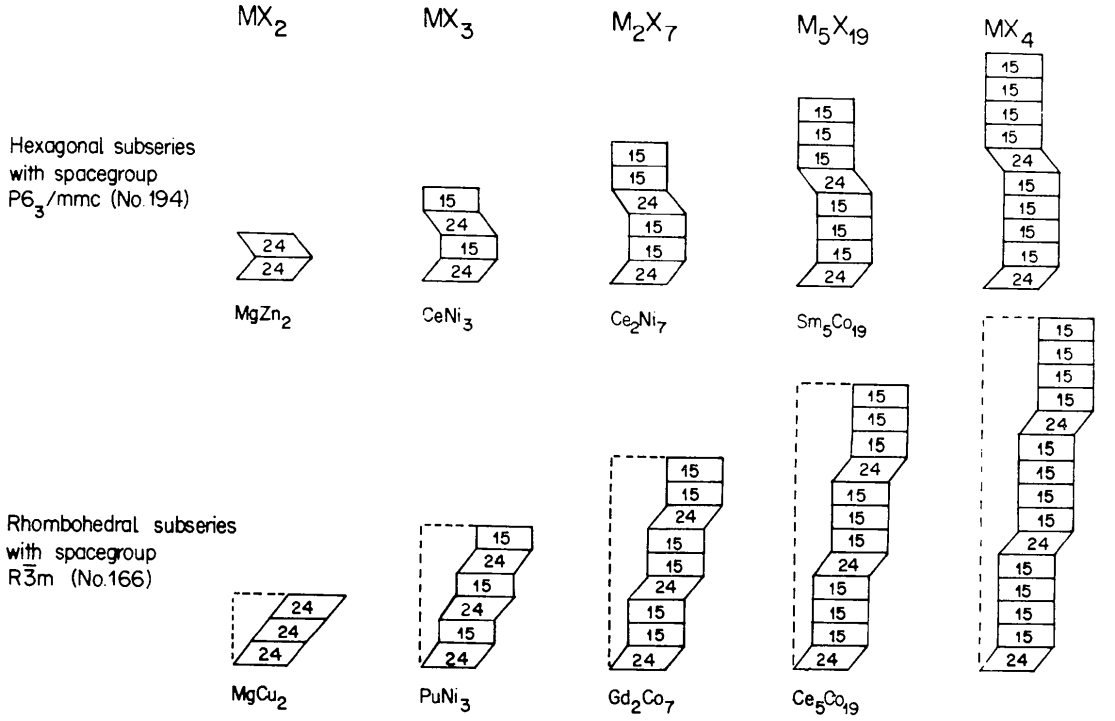

Fig. 5. The crystal structure types of the hexagonal-rhombohedral $M_{n+1}X_{5n-1}$ structure series described by stacking of M_2X_4 and MX_5 structure blocks. 24 denotes an M_2X_4 block and 15 an MX_5 block.

reference atom is at the origin. The stacking of the M_2X_7 structure blocks in the Zr_2Ni_7 structure type is shown in Fig. 6 together with the old and the new monoclinic unit cells. Since the stacked M_2X_7 structure

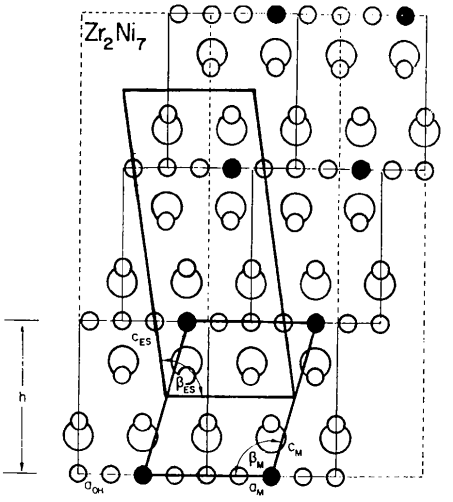

Fig. 6. Block stacking for the monoclinic Zr_2Ni_7 structure type. Eshelman & Smith described the structure with the large unit cell (a_{ES},b_{ES},c_{ES},β_{ES}); it is possible, however, to use a smaller monoclinic cell (a_M,b_M,c_M,β_M).

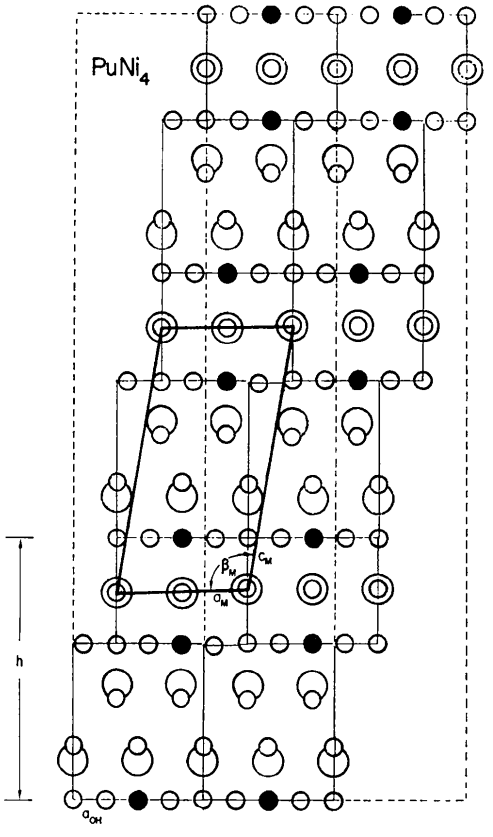

Fig. 7. Block stacking for the monoclinic $PuNi_4$ structure type.

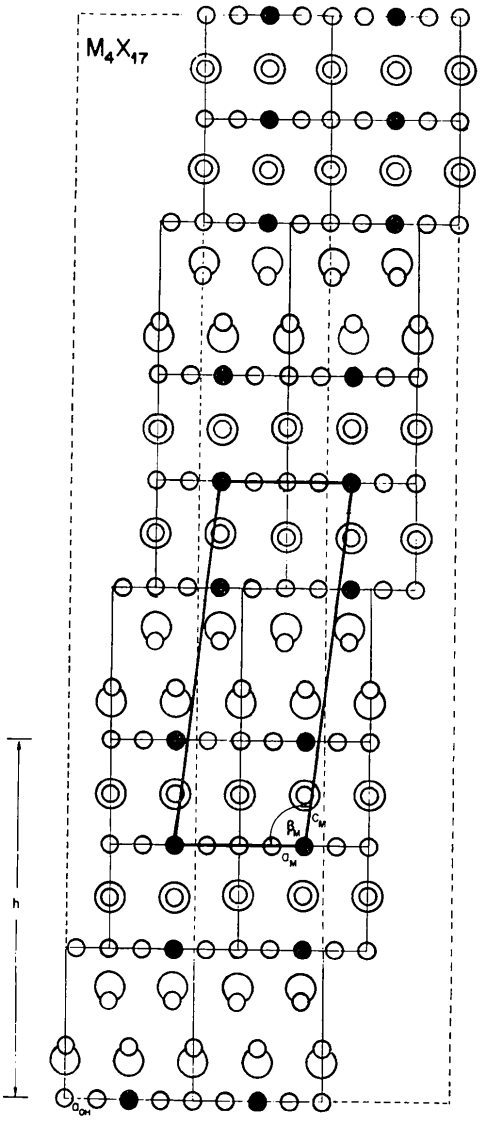

Fig. 8. Block stacking for a hypothetical M_4X_{17} structure, the $n=3$ member of the monoclinic subseries of the $M_{n+1}X_{5n+2}$ structure series.

blocks are translated by $\mathbf{T}_{M_2X_7}=\frac{1}{3}\mathbf{a}_{OH}$ referred to the orthohexagonal axes given in Fig. 2(*c*), a projection of the blocks along $\mathbf{b}_{OH}$ is suitable to present the stacking sequence. The minimum block sequence in this case is a simple M_2X_7 block. Stacking of three blocks leads to an identity period along the pseudohexagonal axis just as in the rhombohedral $M_{n+1}X_{5n-1}$ series. However, since the M_2X_7 block has by itself no hexagonal symmetry, a rhombohedral description as above is impossible. The proper crystallographic unit cell is monoclinic and contains the atoms of a simple M_2X_7 block. If h is the height of the minimum block sequence (here one M_2X_7 block), the dimensions of the monoclinic

Table 4. *The new description of the* Zr_2Ni_7 *structure with the theoretical values given in parentheses*

$C2/m$ (No. 12), $Z=2$
$a_M=4{\cdot}698$, $b_M=8{\cdot}235$, $c_M=6{\cdot}307$ Å, $\beta_M=105{\cdot}92°$ (105·7°)
$b_M/a_M=1{\cdot}753$ (1·732), $c_M/a_M=1{\cdot}342$ (1·235)

	x	y	z
Zr in 4(*i*)	0·393 (0·414)	0	0·729 (0·730)
Ni in 2(*a*)	0	0	0
4(*e*)	$\frac{1}{4}$	$\frac{1}{4}$	0
8(*j*)	0·127 (0·114)	0·165 ($\frac{1}{6}$)	0·344 (0·344)

Table 5. *The structure data for* $PuNi_4$ *after Cromer & Larson* (1960) *with the theoretical values given in parentheses*

$C2/m$ (No. 12), $Z=6$
$a_M=4{\cdot}87$, $b_M=8{\cdot}46$, $c_M=10{\cdot}27$ Å, $\beta_M=100°$ (99·1°)
$b_M/a_M=1{\cdot}737$ (1·732), $c_M/a_M=2{\cdot}108$ (2·033)

	x	y	z
Pu in 2(*a*)	0	0	0
4(*i*)	0·1263 (0·119)	0	0·3552 (0·363)
Ni in 4(*g*)	0	0·3331 ($\frac{1}{3}$)	0
4(*i*)	0·5712 (0·567)	0	0·1987 (0·204)
8(*j*)	0·3199 (0·317)	0·2507 ($\frac{1}{4}$)	0·1993 (0·204)
8(*j*)	0·1422 (0·136)	0·3300 ($\frac{1}{3}$)	0·4066 (0·407)

cell are given by

$$\mathbf{a}_M=-\mathbf{a}_{OH},\ \mathbf{b}_M=-\mathbf{b}_{OH},\ |\mathbf{c}_M|=\sqrt{h^2+\left(\frac{\mathbf{a}_{OH}}{3}\right)^2},$$

$$\tan(\beta_M-90°)=\frac{|\mathbf{a}_{OH}|}{3h}.$$

The idealized point positions for the Zr_2Ni_7 type referred to the proper monoclinic axes have been calculated from Fig. 2(*c*) and added in parentheses to the transformed experimental values given in Table 4.*

The next member in the monoclinic subseries with $n=2$ has the crystal structure of $PuNi_4$. A block stacking for this structure type is shown in Fig. 7. There is an alternation of one M_2X_7 block with one MX_5 block. The experimental unit-cell data and atomic positions are listed in Table 5. The values in parentheses have been calculated assuming ideal block structures with data listed in Figs. 2(*a*) and 2(*c*).

The block stacking of the hypothetical M_4X_{17} structure obtained with $n=3$ is drawn in Fig. 8 and the corresponding monoclinic point positions are given on Table 6. The unit-cell dimensions for higher members of the series can be obtained from the general formulae given in the right-hand part of Table 2. The point positions are easily calculated from Figs. 2(*a*) and 2(*c*).

* These values have been obtained from those given in Fig. 2(*c*) by applying the following procedure: (1) Multiply $x_{orthohex}$ and $y_{orthohex}$ by -1 to assure that the final monoclinic cell has $\beta_M>90°$. (2) Divide normalized z values by $1{\cdot}45_6$ to obtain true z values. (3) Add one third of true z values to the x values to obtain x values which apply to monoclinic unit cell. (4) Add $\frac{1}{2}$ to x values to have a black reference atom at the origin.

The other subseries of the $M_{n+1}X_{5n+2}$ structure series

Whereas in the monoclinic subseries the stacking of M_2X_7 blocks involves only the $\mathbf{T}_{M_2X_7}$ translation, new subseries are generated when successive blocks are not only translated by $\mathbf{T}_{M_2X_7}$ but also rotated by 60°, 120° or 180°. At present no structures of these subseries are known.

Rotation of successive M_2X_7 blocks by 60° leads to a hexagonal subseries in which the structures have space group $P6_122$. But since the identity period along the hexagonal axis is six times the minimum block sequence h, compounds with this hexagonal symmetry are unlikely to be found. Rotation by 120° generates a trigonal subseries with space group $P3_112$. Finally with a rotation by 180° an orthorhombic subseries is obtained with space group *Ccmm*. The block stacking for the orthorhombic M_2X_7 structure is presented in Fig. 9 in projection along $\mathbf{b}_{OH}$. The point positions of the structures with $n=1$, 2 and 3 for the monoclinic, hexagonal, trigonal and orthorhombic subseries are reported in Table 6. As for the $M_{n+1}X_{5n-1}$ series, other subseries can be constructed by assuming more complex stacking sequences of the M_2X_7 blocks.

A graphical survey of possible orthorhombic and monoclinic structure types of the $M_{n+1}X_{5n+2}$ structure series is presented in Fig. 10. Only contour lines of the structure blocks are shown. Referring to the projections along b_{OH} shown in Figs. 2(*a*) and 2(*c*) an MX_5 block may be represented by a rectangle and an M_2X_7 block by a parallelogram, after joining the black

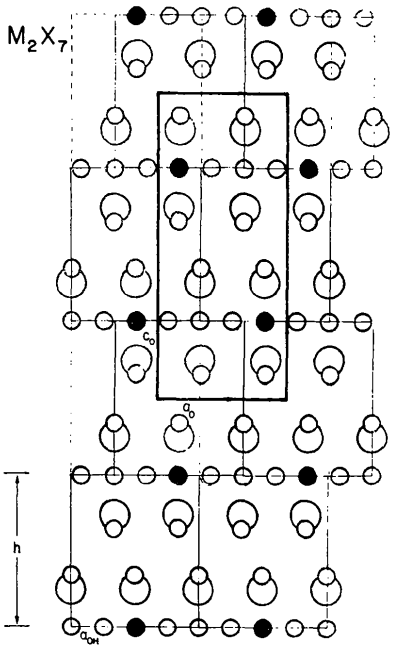

Fig. 9. Block stacking for an orthorhombic M_2X_7 structure, the first member of the orthorhombic subseries.

Table 6. *Calculated structure data for the* $M_{n+1}X_{5n+2}$ *structure series*

Monoclinic subseries
*C*2/*m* (No. 12), $b_M/a_M = \sqrt{3}$

M_2X_7, $n=1$

$c_M/a_M = 1{\cdot}235$, $\beta_M = 105{\cdot}7°$, $Z=2$

			x	y	z
M in	4(*i*)		0·414	0	0·730
X in	8(*j*)		0·114	$\frac{1}{6}$	0·344
	4(*e*)		$\frac{1}{4}$	$\frac{1}{4}$	0
	2(*a*)		0	0	0

Zr_2Ni_7 structure

MX_4, $n=2$

$c_M/a_M = 2{\cdot}033$, $\beta_M = 99{\cdot}1°$, $Z=6$

			x	y	z
M in	4(*i*)		0·119	0	0·363
	2(*a*)		0	0	0
X in	8(*j*)		0·317	$\frac{1}{4}$	0·204
	8(*j*)		0·136	$\frac{1}{3}$	0·407
	4(*g*)		0	$\frac{1}{3}$	0
	4(*f*)		0·567	0	0·204

$PuNi_4$ structure

M_4X_{17}, $n=3$

$c_M/a_M = 2{\cdot}842$, $\beta_M = 96{\cdot}7°$, $Z=2$

			x	y	z
M in	4(*i*)		0·548	0	0·145
	4(*i*)		0·633	0	0·403
X in	8(*j*)		0·048	$\frac{1}{6}$	0·145
	8(*j*)		0·347	$\frac{1}{4}$	0·290
	8(*j*)		0·144	$\frac{1}{6}$	0·434
	4(*e*)		$\frac{1}{4}$	$\frac{1}{4}$	0
	4(*i*)		0·097	0	0·290
	2(*a*)		0	0	0

Hexagonal subseries
$P6_122$ (No. 178)

$c_H/a_H = 7{\cdot}1350$, $Z=6$

		x	y	z
M in	12(*c*)	0	$\frac{1}{3}$	0·2883
X in	12(*c*)	$\frac{1}{3}$	0	0·2761
	12(*c*)	$\frac{2}{3}$	$\frac{2}{3}$	0·2761
	12(*c*)	$\frac{1}{2}$	$\frac{1}{3}$	$\frac{1}{3}$
	6(*a*)	$\frac{5}{6}$	0	0

$c_H/a_H = 12{\cdot}0340$, $Z=18$

		x	y	z
M in	12(*c*)	0	$\frac{1}{3}$	0·2727
	6(*a*)	$\frac{1}{3}$	0	0
X in	12(*c*)	$\frac{1}{3}$	0	0·2655
	12(*c*)	$\frac{2}{3}$	$\frac{2}{3}$	0·2655
	12(*c*)	$\frac{1}{2}$	$\frac{1}{3}$	0·2994
	12(*c*)	0	$\frac{5}{6}$	0·2994
	12(*c*)	$\frac{1}{2}$	$\frac{5}{6}$	0·2994
	12(*c*)	$\frac{1}{3}$	0	$\frac{1}{3}$

$c_H/a_H = 16{\cdot}9330$, $Z=6$

		x	y	z
M in	12(*c*)	0	$\frac{1}{3}$	0·2662
	12(*c*)	0	$\frac{1}{3}$	0·3092
X in	12(*c*)	$\frac{1}{3}$	0	0·2610
	12(*c*)	$\frac{2}{3}$	$\frac{2}{3}$	0·2610
	12(*c*)	$\frac{1}{2}$	$\frac{1}{3}$	0·2851
	12(*c*)	0	$\frac{5}{6}$	0·2851
	12(*c*)	$\frac{1}{2}$	$\frac{5}{6}$	0·2851
	12(*c*)	$\frac{2}{3}$	$\frac{2}{3}$	0·3092
	12(*c*)	$\frac{1}{3}$	0	0·3092
	12(*c*)	$\frac{1}{2}$	$\frac{1}{3}$	$\frac{1}{3}$
	6(*a*)	$\frac{5}{6}$	0	0

Trigonal subseries
$P3_112$ (No. 151)

$c_{TR}/a_{TR} = 3{\cdot}5675$, $Z=3$

		x	y	z
M in	6(*c*)	$\frac{14}{18}$	$\frac{10}{18}$	0·0767
X in	6(*c*)	$\frac{8}{18}$	$\frac{16}{18}$	0·0522
	6(*c*)	$\frac{2}{18}$	$\frac{4}{18}$	0·0522
	6(*c*)	$\frac{14}{18}$	$\frac{1}{18}$	$\frac{1}{6}$
	3(*b*)	$\frac{5}{18}$	$\frac{13}{18}$	$\frac{5}{6}$

$c_{TR}/a_{TR} = 6{\cdot}0170$, $Z=9$

		x	y	z
M in	6(*c*)	$\frac{14}{18}$	$\frac{10}{18}$	0·0455
	3(*b*)	$\frac{14}{18}$	$\frac{4}{18}$	$\frac{5}{6}$
X in	6(*c*)	$\frac{8}{18}$	$\frac{16}{18}$	0·0309
	6(*c*)	$\frac{2}{18}$	$\frac{4}{18}$	0·0309
	6(*c*)	$\frac{5}{18}$	$\frac{10}{18}$	0·0988
	6(*c*)	$\frac{14}{18}$	$\frac{1}{18}$	0·0988
	6(*c*)	$\frac{5}{18}$	$\frac{1}{18}$	0·0988
	3(*b*)	$\frac{9}{18}$	$\frac{10}{18}$	$\frac{5}{6}$
	3(*b*)	$\frac{2}{18}$	$\frac{16}{18}$	$\frac{5}{6}$

$c_{TR}/a_{TR} = 8{\cdot}4665$, $Z=3$

		x	y	z
M in	6(*c*)	$\frac{14}{18}$	$\frac{10}{18}$	0·0323
	6(*c*)	$\frac{14}{18}$	$\frac{10}{18}$	0·1184
X in	6(*c*)	$\frac{8}{18}$	$\frac{16}{18}$	0·0220
	6(*c*)	$\frac{2}{18}$	$\frac{4}{18}$	0·0220
	6(*c*)	$\frac{5}{18}$	$\frac{10}{18}$	0·0702
	6(*c*)	$\frac{14}{18}$	$\frac{1}{18}$	0·0702
	6(*c*)	$\frac{5}{18}$	$\frac{1}{18}$	0·0702
	6(*c*)	$\frac{8}{18}$	$\frac{16}{18}$	0·1184
	6(*c*)	$\frac{2}{18}$	$\frac{4}{18}$	0·1184
	6(*c*)	$\frac{14}{18}$	$\frac{1}{18}$	$\frac{1}{6}$
	3(*b*)	$\frac{5}{18}$	$\frac{13}{18}$	$\frac{5}{6}$

Orthorhombic subseries
Ccmm (No. 63),* $b_O/a_O = \sqrt{3}$

$c_O/a_O = 2{\cdot}378$, $Z=4$

		x	y	z
M in	8(*f*)	$\frac{1}{3}$	0	0·3848
X in	16(*h*)	$\frac{1}{3}$	$\frac{1}{3}$	0·0784
	8(*g*)	$\frac{7}{12}$	$\frac{1}{4}$	$\frac{1}{4}$
	4(*c*)	$\frac{5}{6}$	0	$\frac{1}{4}$

$c_O/a_O = 4{\cdot}011$, $Z=12$

		x	y	z
M in	8(*f*)	$\frac{1}{3}$	0	0·4317
	4(*c*)	$\frac{1}{3}$	0	$\frac{1}{4}$
X in	16(*h*)	$\frac{7}{12}$	$\frac{1}{4}$	0·3518
	16(*h*)	$\frac{1}{3}$	$\frac{1}{3}$	0·4537
	8(*f*)	$\frac{5}{6}$	0	0·3518
	8(*g*)	$\frac{1}{3}$	$\frac{1}{3}$	$\frac{1}{4}$

$c_O/a_O = 5{\cdot}644$, $Z=4$

		x	y	z
M in	8(*f*)	$\frac{1}{3}$	0	0·3223
	8(*f*)	$\frac{1}{3}$	0	0·4515
X in	16(*h*)	$\frac{1}{3}$	$\frac{1}{3}$	0·3223
	16(*h*)	$\frac{1}{3}$	$\frac{1}{3}$	0·4671
	16(*h*)	$\frac{7}{12}$	$\frac{1}{4}$	0·3947
	8(*f*)	$\frac{5}{6}$	0	0·3947
	8(*g*)	$\frac{7}{12}$	$\frac{1}{4}$	$\frac{1}{4}$
	4(*c*)	$\frac{5}{6}$	0	$\frac{1}{4}$

* To allow a better comparison with the other structure types a setting for space group No. 63 different from that given in *International Tables for X-ray Crystallography* has been chosen. The coordinates of equivalent positions for the general point position 16(*h*) are now:

$$\pm(x,y,z),\ \pm(\bar{x},y,\bar{z}),\ \pm(x,y,\tfrac{1}{2}-z),\ \pm(\bar{x},y,\tfrac{1}{2}+z)+[\tfrac{1}{2}\tfrac{1}{2}0].$$

reference atoms. As above, 15 has been printed in the MX_5 blocks and 27 in the M_2X_7 blocks. The sum of the printed ciphers gives the overall composition formula of the particular crystal structure type.

Characterization of the compounds of each series

No matter to what series a compound may belong, it has always been found to crystallize in the form of platelets perpendicular to $\mathbf{c}_{BL}$ along which the layers are stacked. Compounds of the $M_{n+1}X_{5n-1}$ series are tough and brittle whilst those of the $M_{n+1}X_{5n+2}$ series are soft and present a graphite-like texture with cleavage planes perpendicular to **c**. These differences in mechanical properties depend neither on the composition nor on the subseries symmetry. They come from the differences in the building elements of each series *i.e.* M_2X_4 and M_2X_7 blocks.

In MX_5 and M_2X_4 blocks, all atoms are situated in high-symmetry positions. An overlap of *d* orbitals can occur and could be responsible for the brittleness of the $M_{n+1}X_{5n-1}$ compounds. Such enhancement of the metallic bonding is not possible in the $M_{n+1}X_{5n+2}$ series owing to the reduction of symmetry due to the translation $\mathbf{T}_{M_2X_7}$ between the I'' layers. On the basis of a hard-sphere packing model, the M atoms and the X atoms are in contact with like atoms in both M_2X_4 and M_2X_7 blocks. In MX_5 blocks, there is no contact between M atoms, X atoms touching either X atoms or M atoms. However in M_2X_7 blocks, the M atoms are in contact with some X atoms. The shortest interatomic distances in the three blocks are shown in Table 7. The toughness of the MX_5 phase reflects a strong cohesion of the *W* and *I* layers. The substitution in the MX_5 blocks which generates the M_2X_4 blocks introduces contact between M atoms. The I' layers are deformed but keep their cohesion because of the new bonding between M atoms. In the M_2X_7 blocks, the deformation associated with the stacking of the two I'' layers prevents contact between M and X atoms within each I'' layer. Consequently the stability of I'' layers

Table 7. *Interatomic distances in the three structure blocks with the number of neighbours given in parentheses*

X_W belongs to the welding layer, X_I and M_I to an intermediate layer *I*, I' or I''

	MX_5	M_2X_4	M_2X_7
X_W–X_W	(4) 0·5 a_{BL}	(4) 0·5 a_{BL}	(4) 0·5 a_{BL}
X_W–X_I	(4) 0·5 a_{BL}	(2) 0·5 a_{BL}	(4) 0·5 a_{BL}
X_W–M_I	(4) 0·645 a_{BL}	(6) 0·586 a_{BL}	(4) 0·594 a_{BL}
X_I–X_W	(6) 0·5 a_{BL}	(6) 0·5 a_{BL}	(3) 0·5 a_{BL}
X_I–X_I			(2) 0·5 a_{BL}
X_I–X_I	(3) 0·577 a_{BL}	(3) a_{BL}	(3) 0·577 a_{BL}
X_I–M_I			(1) 0·569 a_{BL}
X_I–M_I	(3) 0·577 a_{BL}	(6) 0·586 a_{BL}	(3) 0·584 a_{BL}
M_I–X_W	(12) 0·645 a_{BL}	(9) 0·586 a_{BL}	(6) 0·594 a_{BL}
M_I–X_I			(2) 0·569 a_{BL}
M_I–X_I	(6) 0·577 a_{BL}	(3) 0·586 a_{BL}	(6) 0·584 a_{BL}
M_I–M_J	(2) 0·816 a_{BL}	(4) 0·612 a_{BL}	(2) 0·640 a_{BL}

Table 8. *Axial ratio, conditions for possible reflexions and relations between F(hkl) values for the various structure series, always referred to a hexagonal or pseudo-hexagonal unit cell*

Structure series	Subseries	Idealized c/a ratio $n=1$	$n=2$	$n=3$	$n=4$	n	Conditions for possible reflexions	Relations between $F(hkl)$ values
$M_{n+1}X_{5n-1}$	rhombohedral	2·45	4·89	7·35	9·79	$3n\sqrt{2}/\sqrt{3}$	hkl: $-h+k+l=3n$ only	according to space group $R\bar{3}m$
	hexagonal	1·63	3·27	4·89	6·53	$2n\sqrt{2}/\sqrt{3}$	hhl: $l=2n$ only	according to space group $P6_3/mmc$
$M_{n+1}X_{5n+2}$	monoclinic	3·57	6·02	8·47	10·92	$\frac{2n\sqrt{6}+\sqrt{5}}{2}$	hkl: $-h-k+l=3n$ only	$\lvert F(hkl)\rvert=\lvert F(khl)\rvert$, $\lvert F(hil)\rvert=\lvert F(ihl)\rvert$, $\lvert F(kil)\rvert=\lvert F(ikl)\rvert\neq\lvert F(hkl)\rvert$
	hexagonal	7·14	12·03	16·93	21·89	$2n\sqrt{6}+\sqrt{5}$	$00l$: $l=6n$ only	according to space group $P6_122$
	trigonal	3·57	6·02	8·47	10·92	$\frac{2n\sqrt{6}+\sqrt{5}}{2}$	$00l$: $l=3n$ only	according to space group $P3_112$
	orthorhombic	2·38	4·01	5·64	7·27	$\frac{2n\sqrt{6}+\sqrt{5}}{3}$	hhl: $l=2n$ only	$\lvert F(hkl)\rvert=\lvert F(khl)\rvert$, $\lvert F(hil)\rvert=\lvert F(ihl)\rvert$, $\lvert F(kil)\rvert=\lvert F(ikl)\rvert=\lvert F(hkl)\rvert$

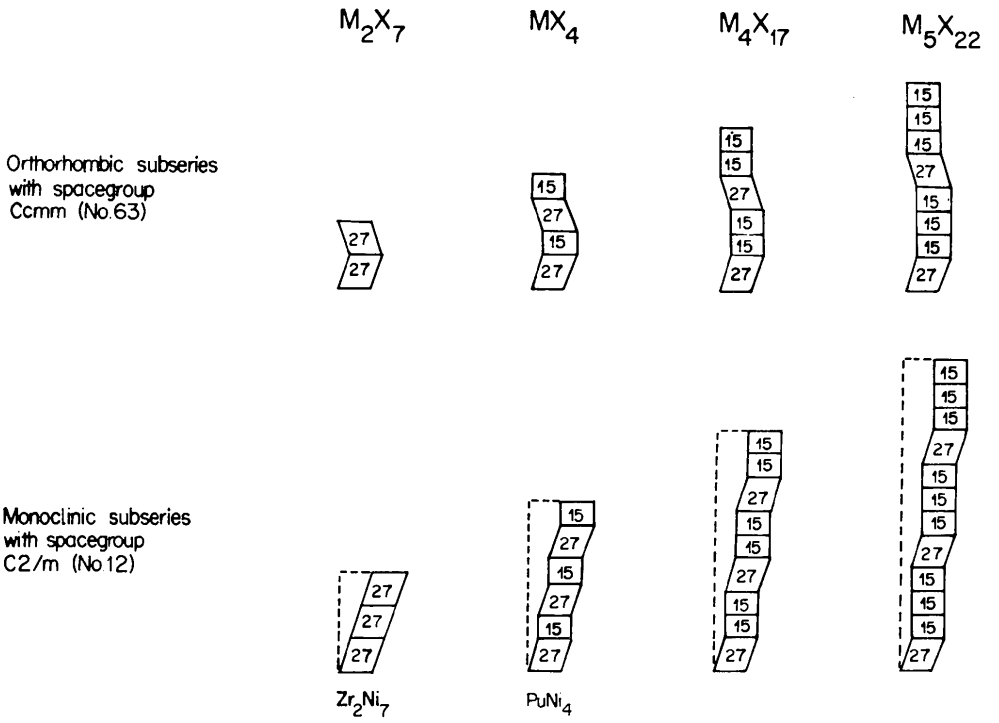

Fig. 10. The orthorhombic and monoclinic crystal structure types of the $M_{n+1}X_{5n+2}$ structure series described by stacking of M_2X_7 and MX_5 structure blocks. 27 denotes an M_2X_7 block and 15 an MX_5 block.

must decrease, giving rise to the observed cleavage planes.

In conclusion, the structure series to which a given crystal belongs can be deduced from the mechanical properties. Weissenberg or precession photographs of the plate-like single crystals should allow a determination of the subseries. It is experimentally convenient to study the hexagonal or pseudo-hexagonal unit cell which has its basal plane parallel to the main plane of the platelet. In Table 8 are given the values for the c/a ratio, condition for possible reflexions and relations between F values for the different subseries, always referred to hexagonal or pseudo-hexagonal axes. Once the type of subseries has been found, the proper crystallographic axes and point positions can be derived from Table 2 and Figs. 2(*a*), 2(*b*) or 2(*c*).

References

BERTAUT, E. F., LEMAIRE, R. & SCHWEIZER, J. (1965). *Bull. Soc. Fr. Minér. Crist.* **88**, 580–585.

CROMER, D. T. & LARSON, A. C. (1959). *Acta Cryst.* **12**, 855–859.

CROMER, D. T. & LARSON, A. C. (1960). *Acta Cryst.* **13**, 909–912.

CROMER, D. T. & OLSEN, C. E. (1959). *Acta Cryst.* **12**, 689–694.

ESHELMAN, F. R. & SMITH, J. F. (1972). *Acta Cryst.* B**28**, 1594–1600.

KHAN, Y. (1974*a*). *Acta Cryst.* B**30**, 1533–1537.

KHAN, Y. (1974*b*). *Phys. Stat. Sol.* (a) **23**, 425–434.

LEMAIRE, R. (1966). *Cobalt*, **33**, 201–211.

OSTERTAG, W. (1967). *J. Less-Common Met.* **13**, 385–390.

SANDS, D. E., ZALKIN, A. & KRIKORIAN, O. H. (1959). *Acta Cryst.* **12**, 461–464.